

Pictures with basic description on Kuramoto-Model Coupling Reconstruction Process

1 General scope of the reconstruction procedure and used notation

In this part of the current paper we provide the description of Kuramoto model, notation for used variables and general description of inverse problem for Kuramoto model being studied.

Let us consider two oscillators with frequencies ω_1 and ω_2 respectively; let $\Omega = \frac{\omega_1 + \omega_2}{2}$ be their synchronised common frequency, thus

$$\begin{cases} \omega_1 &= \Omega + \Delta\omega \\ \omega_2 &= \Omega - \Delta\omega \end{cases},$$

where we denote symmetrical frequency difference as $\Delta\omega$. In order to describe the evolution of their phases $\theta_1(t)$ and $\theta_2(t)$ we propose following differential equations (let us denote the coupling function of oscillators as $k = k(t)$):

$$\begin{cases} \dot{\theta}_1 = \omega_1 + \frac{k}{2} \sin(\theta_2(t) - \theta_1(t)) \\ \dot{\theta}_2 = \omega_2 + \frac{k}{2} \sin(\theta_1(t) - \theta_2(t)) \end{cases},$$

which could be easily transformed by summing and subtracting equations above into the following:

$$\begin{cases} \dot{\theta}_1 + \dot{\theta}_2 = 2\Omega \\ \dot{\theta}_1 - \dot{\theta}_2 = 2\Delta\omega - k \sin(\theta_1(t) - \theta_2(t)) \end{cases}$$

Denoting $\theta = \theta_1 - \theta_2$, we get

$$\dot{\theta} = 2\Delta\omega - k \sin \theta(t) \tag{1}$$

Solving equation (1), the evolution of phase difference can be obtained (assuming the first equation of the system is easily solvable); this states the direct problem in Kuramoto model.

Our paper focuses on the *inverse* problem: considering that the coupling $k(t)$ is generally unknown, let us assume that its approximation $k_0(t)$ can be obtained from the real data (the whole procedure of its extraction and necessary assumptions are not in the scope of this report). Then by solving equation (1) with $k = k_0(t)$ we get the approximation of phase difference $\theta_0(t)$; this can be used to construct two “virtual” oscillators with given phase difference $\theta_0(t)$:

$$\begin{cases} X_0(t) = \sin(\Omega t) \\ Y_0(t) = \sin(\Omega t + \theta_0(t)) \end{cases}$$

Note that proposed virtual oscillators imply that amplitudes of both oscillators are the same; moreover let us compute the sliding correlation $C_0(t)$ between $X_0(t)$ and $Y_0(t)$ over a window of common period of oscillators $T = \frac{2\pi}{\Omega}$:

$$\begin{aligned} C_0(t) &= C_T(X_0, Y_0) = \\ &= \frac{\int_{t-T/2}^{t+T/2} (X_0(\tau) - \langle X_0(\tau) \rangle_T) (Y_0(\tau) - \langle Y_0(\tau) \rangle_T) d\tau}{\sqrt{\int_{t-T/2}^{t+T/2} (X_0(\tau) - \langle X_0(\tau) \rangle_T)^2 d\tau \int_{t-T/2}^{t+T/2} (Y_0(\tau) - \langle Y_0(\tau) \rangle_T)^2 d\tau}}, \end{aligned} \quad (2)$$

where by $\langle X_0(\tau) \rangle_T$ we denote the mean value of $X_0(t)$ over used window.

The main assumption of overseen reconstruction procedure states that the system is close to its stationary state; in which case the sliding correlation between oscillators can be computed as $\theta_0(t) = \arccos C_0(t)$. So in case of quasi-stationarity new reconstructed phase difference $\varphi(t)$ can be obtained using $C_0(t)$ computed by equation (2):

$$\varphi(t) = \arccos C_0(t)$$

Using that $\dot{\varphi} \approx 0$ one could substitute θ with φ in the equation (1) and find reconstructed coupling $\hat{k}(t)$:

$$\hat{k}(t) = \frac{2\Delta\omega}{\sin \varphi(t)}$$

Note that described procedure is proved to be correct in case

$$|k_0(t)| \geq 2\Delta\omega \quad (3)$$

which is referred as *the main Kuramoto inequality*.

2 Model functions and reconstruction

In this part of our research we investigate the proposed reconstruction procedure from qualitative and quantitative (we describe used metrics further) points of view for 4 different sets of coupling approximations $k_0(t)$: piecewise-constant, sine, autoregressive approximations and its combination; focusing on the case of temporarily breaking the main Kuramoto inequality (3).

2.1 Piecewise-constant approximations

In this case we assume that $k_0(t)$ can be described as

$$k_0(t) = \begin{cases} d, & t < T_0 \vee t > T_0 + s \\ d + \Delta d, & T_0 \leq t \leq T_0 + s \end{cases}$$

where Δd can be either positive or negative; we refer to the period of the second value $d + \Delta d$ as the shock period.

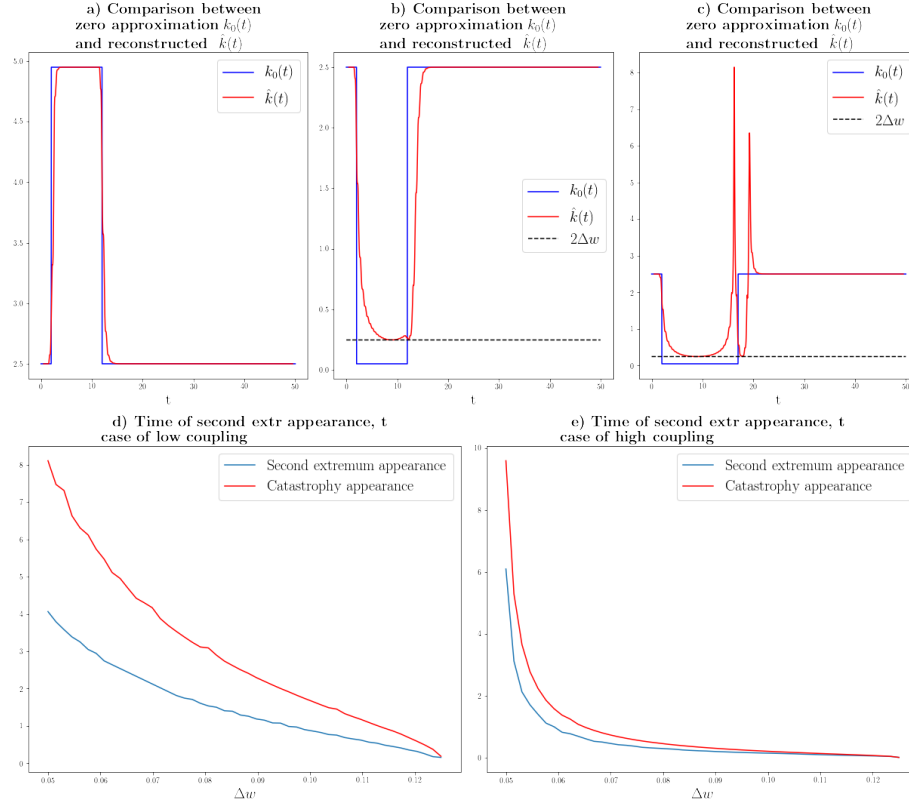


Figure 1: Reconstruction of piecewise-constant approximation $k_0(t)$: examples and length of the period with shock corresponding to the second extremum and singularity appearances

Figures (1a–c) illustrate results of reconstruction of single approximation in three different cases: without breaking the main Kuramoto inequality (1a); breaking Kuramoto inequality with resulting additional extremum appearance after the shock period (1b); and breaking Kuramoto inequality with resulting appearance of singularity in reconstructed function (1c).

In case of (1a) it can be seen that the system relaxes to the shocked value during the shock period and to the normal value after the shock significant

amount of time (measured in common periods of oscillators); thus one can say that the system has a noticeable “memory”. As for the effects of breaking the main Kuramoto inequality (among cases in which the shock period is not long enough to create qualitatively new figures) we outline two different scenarios: if the shock period is long enough (consider figures (1d–e) in order to establish the appropriate length) reconstructed function tends to begin a relaxation to the normal value even before the shock period is over thus creating the second extremum after the shock; in case when the system has enough time to fully relax to the normal value during the shock, the reconstruction process results into the singularity in $\hat{k}(t)$ (specifically this means that in that moment of time oscillators are fully uncorrelated).

For the further investigation of this phenomena we provide figures (1d–e) devoted to establishing the length of the shock period s towards $\Delta\omega$ sufficient for the second extremum and singularity; to give more sophisticated picture we study cases of low coupling (low d , comparatively to $2\Delta\omega$) (fig. 1d) and high coupling (fig. 1e). As shown increasing (and therefore strengthening the breaking difference in the inequality) symmetrical phase difference results into earlier appearance of both effects and shorter time interval between the second extremum appearance and the singularity.

2.2 Sine approximations

In this part we propose coupling approximation as follows:

$$k_0(t) = A \sin(Bt + \varepsilon) + C,$$

where A is an amplitude, B is a frequency and C is a mean value. Moreover, unless stated otherwise, consider $C - A < 2\Delta\omega$, so we study mainly the case of inequality breaking.

Same as for piecewise-constant case, figures (2a–c) illustrate results of reconstruction of single approximation; for those pictures we vary the frequency of sine being reconstructed. Figure (2a) shows the case for correct reconstruction despite the inequality breaking; similar to the piecewise-constant case (fig. (1b)) we observe gradual relaxation to values restricted by inequality with noticeable flattening. Figures (2b) and (2c) shows two opposite cases of poor reconstruction quality: for the figure (2b) it can be seen that more frequent fluctuation are less appropriate for the reconstruction which can be explained by an absence of sufficient time for relaxation as seen on fig. (1) and (2a); figure (2c) demonstrates the case of singularity achieved by the same condition as on fig. (1c) — too long restricted value period.

Figures (2d–e) generalize the study of reconstruction towards approximation’s sine frequency; to measure the quality of the process we propose the following metric:

$$R_0[\hat{k}, k_0] = \frac{\int_0^L (k_0(t) - \langle k_0(t) \rangle_L) \left(\hat{k}(t) - \langle \hat{k}(t) \rangle_L \right) dt}{\int_0^L k_0^2(t) dt}$$

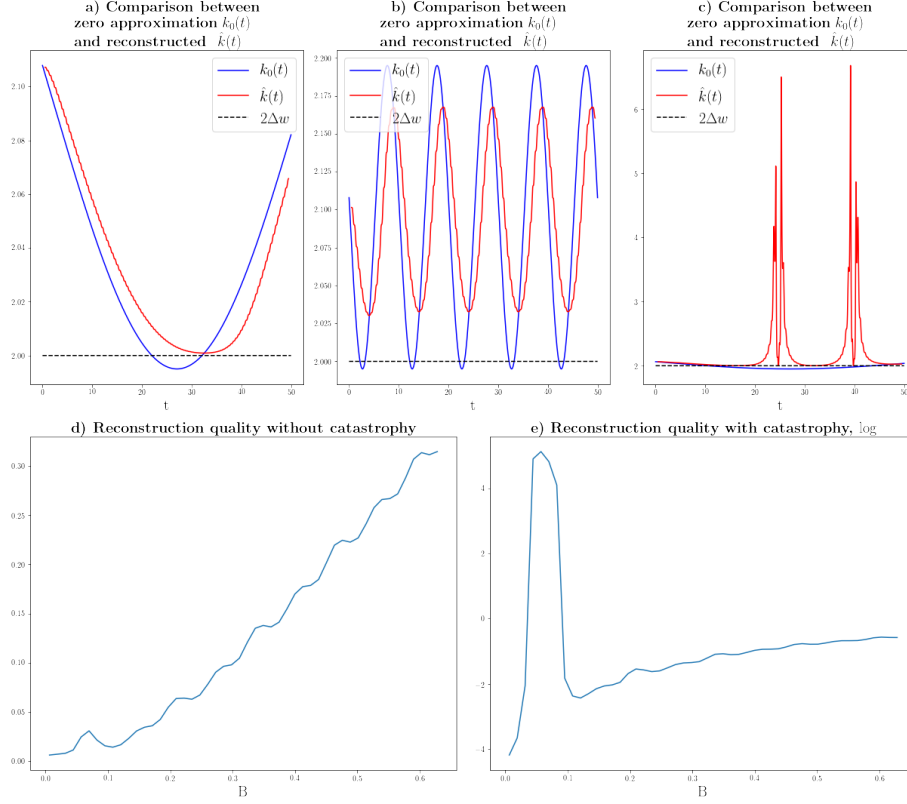


Figure 2: Sine approximations of $k_0(t)$: examples and quality of reconstruction towards sine frequency

(in assumption that $t \in [0; L]$ so L denotes the end of time interval being studied). Figure (2d) illustrates the case of $C - A > 2\Delta\omega$; thus general increase of error corresponds with phenomenon observed on fig. (2b). Figure (2e) explores the case of $C - A < 2\Delta\omega$ (in log scale): here we can see three different parts — the first one corresponds to the case of no breaking (such as fig. (2d)), then we obtain highly unreconstructed part corresponding to fig. (2c) associated with singularities and finally we get similar to fig. (2d) plot explained by increase of sine frequency.

2.3 Autoregressive random approximations

In order to simulate the random noise for our procedure we study autoregressive process (AR(1)), which can be described as:

$$k_0(t_n) = \alpha k_0(t_{n-1}) + \xi_n,$$

where $\xi_n \sim \mathcal{N}(\mu, \sigma)$ and $0 < \alpha < 1$. This stochastic process is widely on as

weakly stationary after $n = \frac{1}{1-\alpha}$ with the mean equal to $\frac{\mu}{1-\alpha}$ and the standard deviation equal to $\frac{\sigma^2}{1-\alpha^2}$.

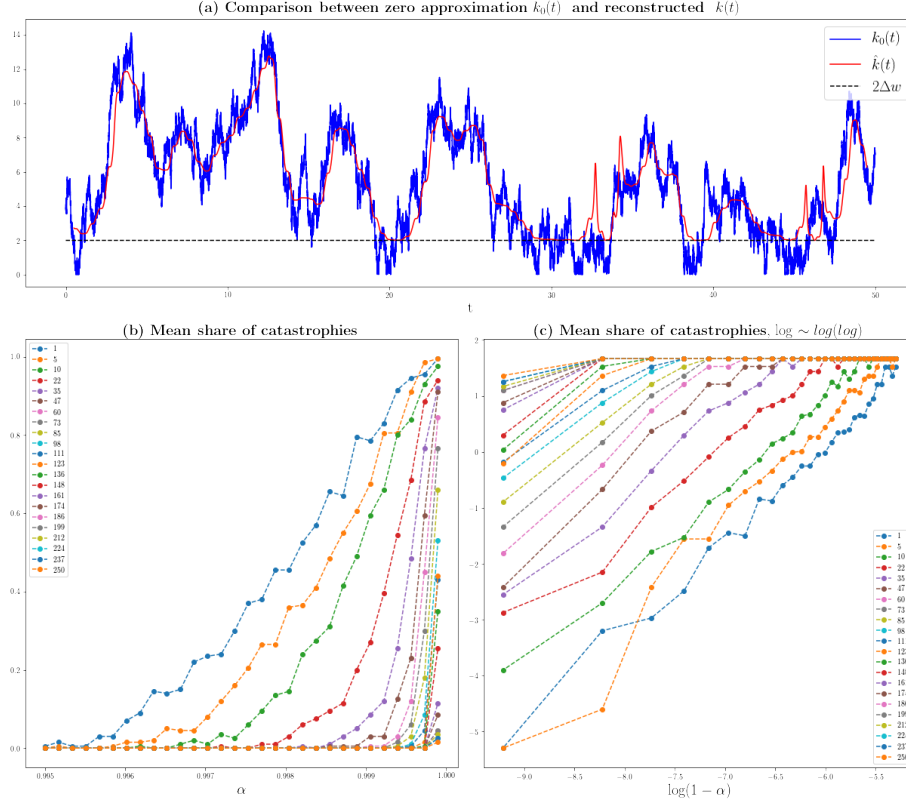


Figure 3: Autoregressive approximations of $k_0(t)$: an example and the probability of singularity towards α and μ

One realization of described process and its reconstruction are shown on figure (3a); more precisely, in that case we obtain the general understanding of reconstruction as smoothing highly variable approximations; furthermore it can be seen that for the time interval in around $t \approx 15$ we get poor reconstruction quality explained by rapid change of $k_0(t)$ as for too frequent sine series as in fig. (2b); for the time interval in around $t \approx 20$ we get a correct reconstruction with flattening similar to fig. (2a); the time interval for $t \approx 32$ illustrates the occurrence of singularity with the same reasoning as for piecewise-constant and sine cases.

According to the stochasticity of the process one should assume that for every set of parameters all seen for previous functions cases of reconstruction are possible with some probability. Thus we vary α and μ on figure (3b-c) in order to get the probability of singularity in each case (the mean $\mu = 2\Delta\omega + K\sigma$ is varied

through K). As shown on figure (3b) it can be concluded that the probability of obtaining singularity through the reconstruction declines with the mean growth which can be explained by the fact that with the mean growth expected values of the stochastic process are more distant from $2\Delta\omega$ with fixed variance; thus prolonged restricted values of the process are less likely. Another trend of figure (3b) is general growth of singularity probability towards α ; specifically, as shown in figure (3c) in $\log X \sim \log \log Y$ scale, it is linear with regression coefficient equal to 1 (with non-distinctive fluctuations). One should notice that whilst being linear in $\log X \sim \log \log Y$ scale, given plot is not linear in simpler $X \sim \log Y$ scale; it can be explained by the presense of pre-exponential functional factor $f(\alpha)$ that gets close to constant only in $\log X \sim \log \log Y$ scale.

2.4 Noised sine approximation and CIs

The last family of model functions used as $k_0(t)$ approximation is the combination of simple sine approximation with random additive noise described above; precisely

$$k_0(t) = A \sin(Bt + \varepsilon) + C + X(t_n),$$

where $X(t_n) = \alpha X(t_{n-1}) + \xi_n$, $\xi_n \sim \mathcal{N}(0, \sigma)$, $0 < \alpha < 1$.

In this scope for given problem the main question one should answer is how influential the additive autoregression process is; in other words we should establish the confidence interval associated with random noise for reconstructed function $\hat{k}(t)$; let us denote the width of the confidence interval as $e(t)$. For figures (4a,c) we determine 95% confidence interval for each moment of time (note that there is no given knowledge about the distribution); also we provide de-noised $k_0^{clear}(t)$ and $\hat{k}^{clear}(t)$ in order to illustrate centers of confidence interval and describe overall reconstruction error.

Figures (4a–b) demonstrates the case of varying σ in additive noise; for each case figure (4b) shows the corresponding plot $e(t)/(\sigma \cdot k_0^{clear}(t))$. Therefore it can be concluded that the width of confidence interval is proportional to the noise's variance; in the same time plots discrepancies correspond to lower phases of the de-noised sine series where as seen on fig. (3b) the probability of singularity occurrence is higher thus making reconstruction mostly incorrect and more variable. Figures (4c–d) compiled similarly to figures (4a–b); note that in this case we vary the Kuramoto inequality threshold $\Delta\omega$ and since figure (4c) does not demonstrate any difference in confidence interval's widths towards the threshold, we use only $e(t)/k_0^{clear}(t)$ for figure (4d). Note that the case of $\Delta\omega = 0.15$, which implies not only random breaking of the main Kuramoto inequality but also systematical breaking as shown on figure (4c) with yellow dashed line, noticeably differs from the others; despite the fact that it is seemingly more probable case for singularity occurrence, the plot is lower than the others which can be explained by the fact that not only we obtain singularity and incorrect reconstructions but we also obtain correct ones with flattening (as discussed earlier) to $2\Delta\omega$ thus making reconstructed function less variable resulting in more narrow confidence interval.

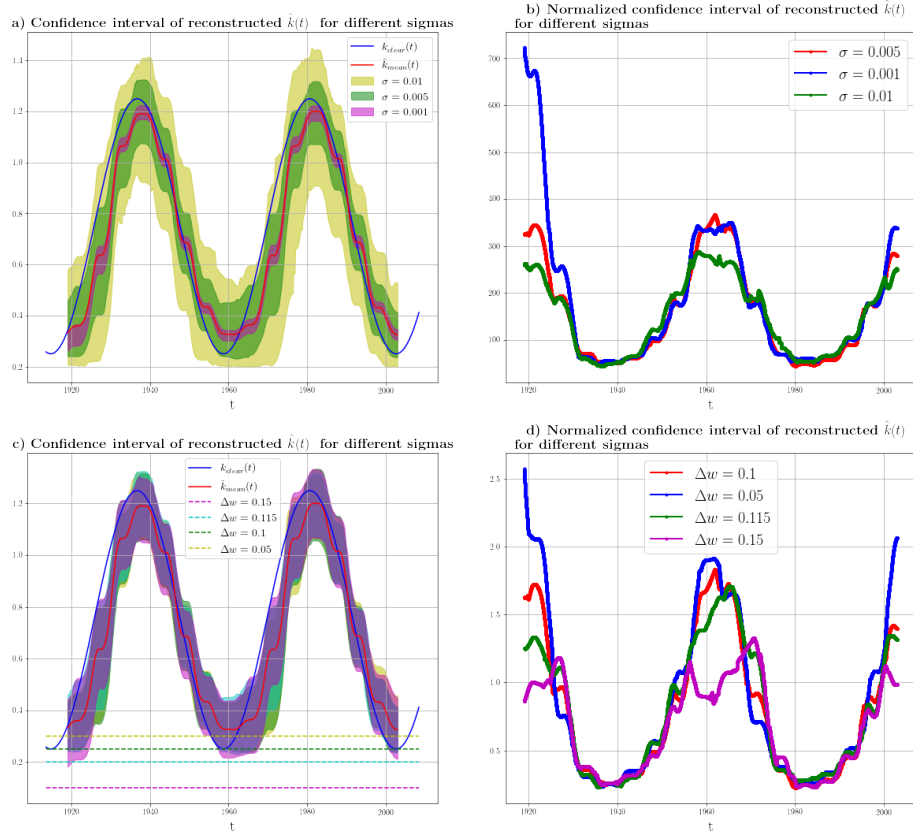


Figure 4: Sine approximations of $k_0(t)$ with additive autoregressive noise: varying σ and $\Delta\omega$